Journal of Engineering Mathematics 19 (1985) 341–349.

Thick waterfalls from horizontal slots

K.H.M. GOH and E.O. TUCK

Applied Mathematics Department, University of Adelaide, Adelaide S.A. 5001, Australia

(Received June 12, 1985)

Summary

A numerical investigation is made of the two-dimensional steady, irrotational flow of a jet of water falling under the influence of gravity, from a channel with an upper wall. This non-linear problem is formulated as an integro-differential equation for the two free surfaces of the jet, via a hodograph transformation, and this equation is then discretized to yield a finite set of non-linear equations which are solved numerically by Newton's method. Physically meaningful solutions are found to exist only for Froude numbers F greater than or equal to a certain critical value F_0, which is to be determined. Results are presented, both for $F > F_0$ where the detachment is with continuous slope and for $F = F_0$, where the upper detachment point is a stagnation point at a 120° corner.

1. Introduction

Numerical solutions for thick waterfalls have been obtained by Chow and Han [1] using a finite difference scheme and by Smith and Abd-el-Malek [4] via integral equations derived by Hilbert's method. Integral equations were also employed by Vanden-Broeck and Keller [6] for a free jet. This latter approach is again called upon in this study, to provide further results for a generalisation of the waterfall problem to allow for an upper upstream boundary.

Specifically, we assume that there is an incident uniform stream U, initially bounded by two horizontal walls of width w apart, the ends of which are in general offset from each other. In the limit as the end of the top wall is moved a large distance upstream of the end of the bottom wall, the classical waterfall problem is recovered. Of particular interest is when we have zero offset, which is equivalent to efflux from a straight nozzle.

It is convenient to parameterize the problem by the Froude number $F = U/\sqrt{gw}$, and, in principle, this and the above-mentioned previous studies are intended to provide solutions for arbitrary input F values. The complexity of the computational task is such that only one or two special values of F have been solved for in the past, but we provide a large collection of solutions here. In addition to the numerical work at finite F, there is a substantial body of literature (e.g. Clarke [2], Tuck [5], Geer and Keller [3]) on thin waterfalls or free jets, i.e. on the asymptotic limit as F tends to infinity.

In the present case, at any fixed nozzle geometry with finite offset, physically realistic solutions can only be found for $F \geqslant F_0$, where F_0 is determined here. This means that if we decrease F from infinity, so allowing the jet to become thicker and thicker, no solution exists below a critical Froude number F_0. This threshold value is dependent on the nozzle offset, and, for example, when the offset is zero, $F_0 = 0.551$. Solutions for $F > F_0$ have the property that the free steamlines detach smoothly and horizontally from the walls. However, as F tends to F_0, a stagnation point develops at the upper detachment point, at which the free streamline makes an angle of 120° with the upper wall, i.e. descends at 60° to the horizontal initially.

2. Mathematical formulation

The flow of interest is sketched in Figure 1, in a non-dimensional coordinate system such that at upstream infinity there is a uniform stream of unit magnitude, in a horizontal channel of unit width. That channel ends near $x = 0$, and the resulting stream of water then falls forever under gravity. The walls of the channel need not end at the same value of x. We let the upper and lower walls end at $(l, 0)$ and $(0, -1)$ respectively, where l is the amount of overhang relative to the slot width, which may be positive as in Figure 1, or negative, or zero.

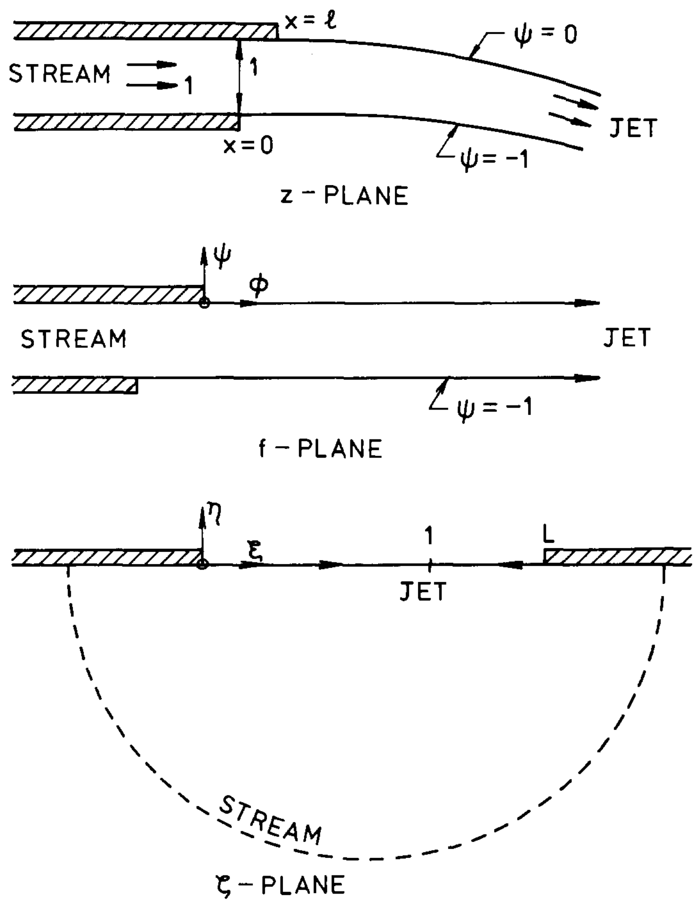

Figure 1. Problem definition and conformal-mapping sketches.

In terms of a stream function ψ, the upper streamline is taken as $\psi = 0$, and the lower as $\psi = -1$. Wherever these streamlines are free, namely $x > l$ for the upper and $x > 0$ for the lower, the pressure must be atmospheric, a condition which, when coupled with Bernoulli's equation, yields the non-dimensional equation

$$yF^{-2} + \tfrac{1}{2}q^2 = \text{constant}, \tag{2.1}$$

where q is the flow speed.

We choose to seek an analytical function $z = z(f)$, where $z = x + \mathrm{i}y$ and $f = \phi + \mathrm{i}\psi$ is a complex velocity potential. The strip $-1 < \psi < 0$ in the f-plane can be mapped conformally to the lower half ζ-plane, where

$$\zeta = 1 - \mathrm{e}^{-\pi f} \tag{2.2}$$

as is indicated in Figure 1, and $\zeta = \xi + \mathrm{i}\eta$ will be used here as the fundamental independent variable. As dependent variable, it is convenient to work with the logarithmic hodograph variable

$$\Omega = \tau - \mathrm{i}\theta = \log(\mathrm{d}f/\mathrm{d}z) \tag{2.3}$$

noting that $\tau = \log q$, and θ measures the angle of inclination between a streamline and the x-axis. The free-surface condition (2.1) can be differentiated with respect to ϕ or ξ on $\eta = 0$ to give

$$\pi(1-\xi)\,\mathrm{e}^{3\tau}\frac{\partial \tau}{\partial \xi} + F^{-2}\sin\theta = 0, \quad 0 < \xi < L. \tag{2.4}$$

The edges of the channel are chosen as $\xi = 0$ and $\xi = L$; for any given values of the (real positive) parameters F and L, the actual offset l will be determined by the solution.

In view of the fact that $\Omega = \Omega(\zeta)$ is analytic in the lower half ζ-plane, tends to zero as $|\zeta| \to \infty$, and possesses only integrable singularities, use of Cauchy's theorem shows that, on the real axis $\zeta = \xi - \mathrm{i}0$, its real and imaginary parts are Hilbert transforms of each other. Specifically, we have

$$\tau(\zeta) = \frac{1}{\pi}\int_0^L \frac{\theta(\xi)}{\xi - \zeta}\,\mathrm{d}\xi \tag{2.5}$$

when ζ is real, the integral being of principal-value type if $0 < \zeta < L$. In obtaining (2.5) from Cauchy's theorem, we have used the fact that $\theta = 0$ on the horizontal walls of the channel, i.e. for $\xi < 0$ and $\xi > L$.

If τ is eliminated between (2.4) and (2.5), there results a non-linear integro-differential equation for the unknown function $\theta(\xi)$, $0 < \xi < L$, and our computational effort is reduced to solving that equation with the θ values as our fundamental unknowns. Once $\theta(\xi)$ and hence $\tau(\xi)$ is determined, the actual free-surface profile follows by integration of (2.3), i.e. by evaluating the integrals

$$x(\zeta) - l = \int_0^{\zeta} \mathrm{e}^{-\tau(\xi)}\frac{\cos\theta(\xi)}{\pi(1-\xi)}\,\mathrm{d}\xi \tag{2.6}$$

and

$$y(\zeta)=\int_0^{\zeta} e^{-\tau(\xi)}\frac{\sin\theta(\xi)}{\pi(1-\xi)}\,d\xi, \tag{2.7}$$

with l finally determined by setting $x(L)=0$.

There is a difficulty with the above formulation, exemplified by the fact that the trivial uniform flow $\theta(\xi)\equiv\tau(\xi)\equiv 0$ appears to satisfy (2.4) and (2.5). In fact, because of the loss upon differentiation of the constant on the right-hand side of (2.1), the system (2.4), (2.5) by itself does not possess a unique solution. Uniqueness is restored by noting that (2.7) must yield $y(L)=-1$, and that this is true if

$$\tfrac{1}{2}\,e^{2\tau(0)}=\tfrac{1}{2}\,e^{2\tau(L)}-F^{-2}. \tag{2.8}$$

Equation (2.8) is a necessary subsidiary condition, and the combined system (2.4), (2.5), (2.8) appears to possess a unique non-trivial solution. Note that (2.8) is a direct consequence of (2.1), and in effect guarantees that the pressure on both streamlines is the same.

3. Numerical method

Our major task is to approximate the integral (2.5), replacing it by a summation over, say, N discrete values of $\theta(\xi)$. In order to accomplish this, we need to partition the interval $0\leqslant\xi\leqslant L$ into N segments, the jth segment being $\xi_{j-1}\leqslant\xi\leqslant\xi_j$. This partition must be chosen very carefully, since it must accommodate square-root singularities in $\theta(\xi)$ at the ends, $\xi=0$ and $\xi=L$, and a logarithmic singularity at $\xi=1$. We therefore set

$$\xi_j=\begin{cases}1-e^{-j^2\alpha}, & 0\leqslant j\leqslant M-1\\ 1+(L-1)\,e^{-(N-j)^2\beta}, & M\leqslant j\leqslant N\end{cases} \tag{3.1}$$

for some positive constants α, β. This assigns $M-1$ segments to the upper free surface $0\leqslant\xi<1$, and $N-M$ to the lower $1<\xi\leqslant L$. The Mth segment is special, in that it spans the singularity at $\xi=1$ representing the ultimate free-falling jet. We choose the parameters α and β so that this special segment is symmetric about $\xi=1$, and of width 2ϵ, i.e.

$$\epsilon=e^{-\alpha(M-1)^2}=(L-1)\,e^{-\beta(N-M)^2}, \tag{3.2}$$

where ϵ is an input parameter. The smaller the value of ϵ, the further does the partition of segments extend along the ultimate jet.

Having fixed this partition, we can now discretize the problem in various ways, by local approximation to $\theta(\xi)$ on each separate segment. We choose here the simplest such approximation, by setting $\theta(\xi)=\theta_j=$ constant on the jth segment. The special nonuniform partition (3.1) is designed to "follow" variations in $\theta(\xi)$, so that this step-function approximation retains accuracy even near the singularities. Clearly, this fails as an approximation to $\theta(\xi)$ at $j=M$, since this special segment spans a singularity in which $\theta(\xi)$ possesses a finite but sharp "spike", as is seen in Figure 2. Nevertheless, as a representation of the contribution of such a segment to the integral (2.5), the approximation $\theta\simeq\theta_M=$ constant is still valid, since this spike contributes negligibly to the integral.

Now if $\theta(\xi)$ is so represented in step-function form, the integral (2.5) becomes (without further approximation)

$$\tau(\zeta) = \sum_{j=1}^{N} \theta_j \frac{1}{\pi} \log \left| \frac{\xi_j - \zeta}{\xi_{j-1} - \zeta} \right|. \tag{3.3}$$

All that remains is to substitute (3.3) directly into the boundary condition (2.4) and to force (2.4) to hold at a suitable set of values of ζ.

In practice, we do this at the $N-1$ "pseudo mid-points" of the ith interval, $i \neq M$, defined by setting $j = i - 1/2$ in (3.1). This would be inappropriate at $i = M$, since the mid-point of that interval is the singular point $\zeta = 1$. Instead, the Mth equation is just the subsidiary condition (2.8), in which $\tau(0)$ and $\tau(L)$ are approximated by (3.3) evaluated at the pseudo mid-points of the segments $j = 1$, N respectively. Thus, we now have N non-linear algebraic equations in N unknowns $\theta_1, \theta_2, \cdots, \theta_N$, and solve this system by Newton's method on a VAX 11/780 computer.

Generally, the program was started at a large value of F and with an initial empirical estimate for the θ_j. After convergence is achieved at this F, the new θ values are used as a starting guess for a smaller value of F, and so on. Most results were computed with $N = 60$, $M = 30$ and $\epsilon = 10^{-8}$, and convergence of Newton's method at fixed N to at least six-figure accuracy was achieved in 5 or 6 iterations. The discretization error can then be reduced by increasing N, but the above values are sufficient to give results of three to four-figure accuracy. The only reason for using such a small value of ϵ is to yield an adequate graph of the ultimate jet; a much larger value would suffice numerically.

The x and y coordinates of the free surfaces are computed in a post-processing phase, using the same step-function approximation. That is, the integrals (2.6), (2.7) are approximated by assuming that both θ and τ are constant over the jth interval. This works well for $0 < \zeta < 1$, for the upper free surface. To avoid having to integrate through the singularity at $\xi = 1$ when $\zeta > 1$, we first compute the lower free-surface shape relative to the lower detachment point, then find the x-wise offset l of that point relative to the upper detachment point by integrating upstream. To do this, we use (2.6) to evaluate $x(\zeta) - l$ on the upper wall for $\zeta < 0$, stopping when the flow is essentially uniform ($\phi \sim -4$ or $\zeta \sim -10^5$). We then assume that the same x-value applies to the lower wall at the same choice of ϕ, e.g. at $\zeta \sim +10^5$. Now we integrate again along the lower wall for decreasing positive values of ζ until we reach the lower detachment point at $\zeta = L$.

4. Discussion of results

Figure 2 shows a typical set of primary outputs from the converged Newton iteration process, namely results for $\theta(\xi)$ for various F values, at $L = 2$. Note that the spike $\theta = -\pi/2$ at $\xi = 1$ is very sharp at all Froude numbers. When $F = \infty$, i.e. there is no gravity, the stream is undisturbed, and $\theta \equiv 0$. As F decreases, and the jet is more influenced by gravity, it falls faster, and θ takes more-negative values.

The approach of the θ-values to zero at the ends of the interval, e.g. as $\xi \downarrow 0$, is in general like $\xi^{1/2}$, but as F decreases, the fall is more and more rapid near $\xi = 0$, and eventually a minimum Froude number $F = F_0$ is reached, at which commencement with $\theta(0) = 0$ is impossible. For F values close to F_0, θ is not monotone decreasing in $0 < \xi < 1$,

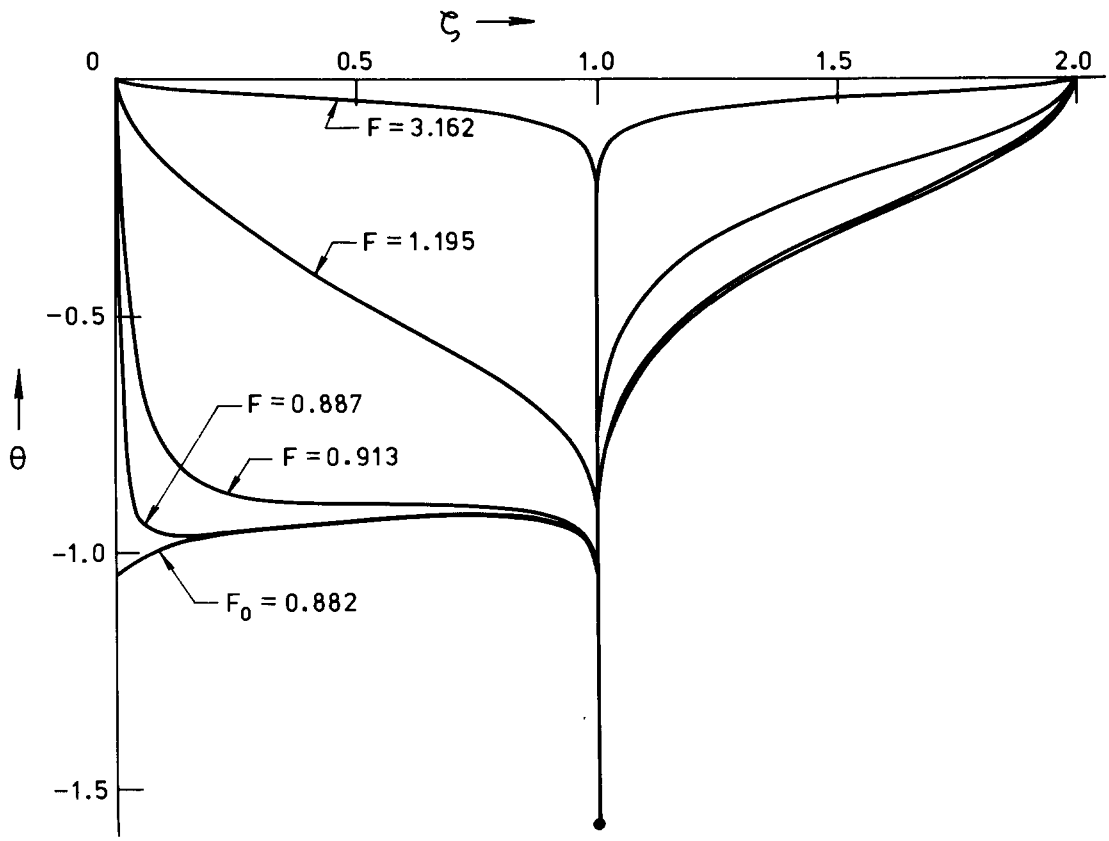

Figure 2. Graph of $\theta(\zeta)$ for various F, at $L = 2$.

but instead takes first a minimum then a maximum value; this corresponds to upper free surface profiles with two inflexion points. As $F \downarrow F_0$, the minimum value of θ approaches $-\pi/3$, and occurs closer and closer to $\xi = 0$.

Because of this rapid change near $\xi = 0$, it is difficult to retain good accuracy with above-described program as $F \downarrow F_0$. However, results at $F = F_0$ itself can be obtained to good accuracy by a simple modification of the program. At $F = F_0$ we now demand that $\theta \to -\pi/3$ as $\xi \to 0$, and enforce this simply by setting $\theta_1 = -\pi/3$ in the discretized system. Having thus eliminated one of our N unknowns, we replace it by treating the Froude number F itself as an unknown. The converged Newton iterations for this modified program therefore yield not only an appropriate stagnation-point type flow, but also explicit and accurate estimates of the minimum Froude number F_0. The curve for $F = F_0 = 0.882$ in Figure 2 was computed in this way.

Since the value for L is fixed at 2 in Figure 2, each separate value of F corresponds to a different value of the physical-plane offset l. However, by repeating the computations for a large range of values of L at any F, we can achieve any desired value of l. Figures 3, 4 and 5 show the final free-surface profiles for $l = 0.5$, 0 and -0.5 respectively, for various F. The flow patterns in Figure 3 are typical of the overhang situation, and, as F decreases toward the minimum value of $F_0 = 0.737$, the jet falls more rapidly under gravity, in a smooth and monotone manner.

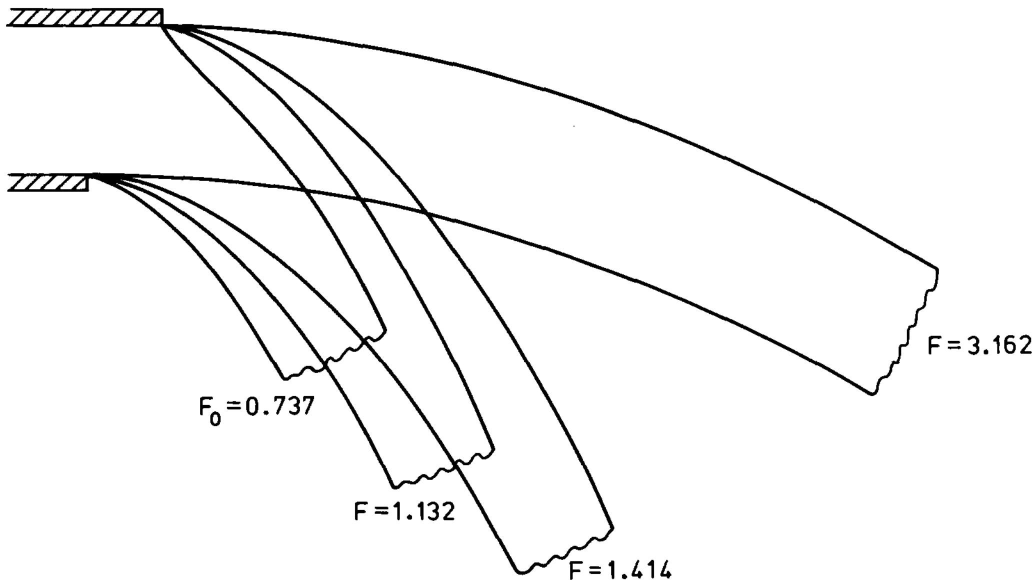

Figure 3. Overhang profile for various Froude numbers.

The results in Figure 4 for the zero-offset case $l = 0$ are of particular interest, since they can represent flow from a straight-ended nozzle, or from a slot in a vertical wall. Here the minimum Froude number is $F_0 = 0.551$. As F decreases, the free jet falls under gravity as is expected, with the curvature of the upper free surface increasing. Close to the stagnation value of $F = 0.551$, the flow still detaches itself horizontally and smoothly from the top

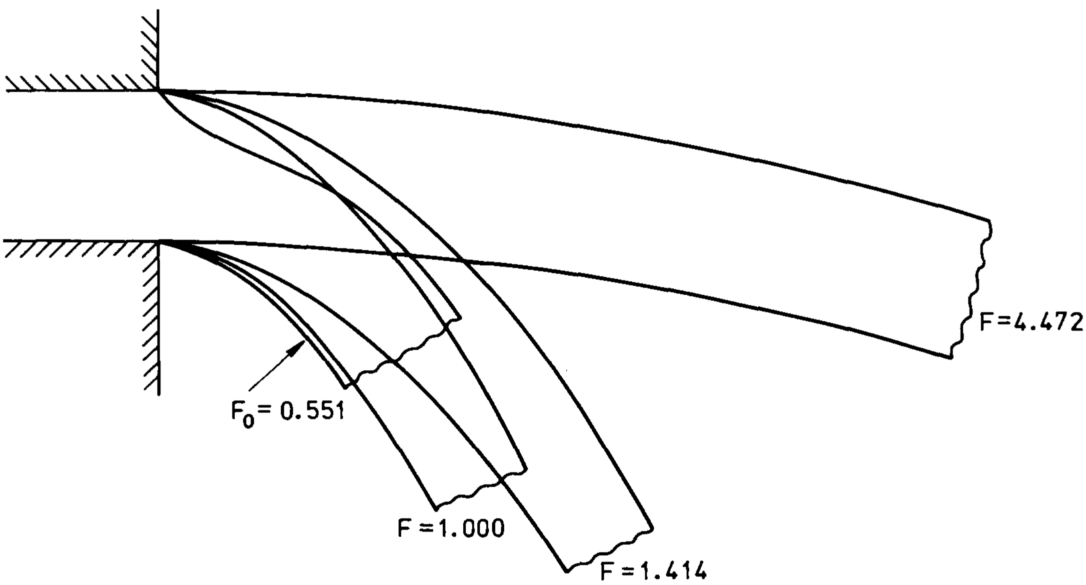

Figure 4. Slot profile for various Froude numbers.

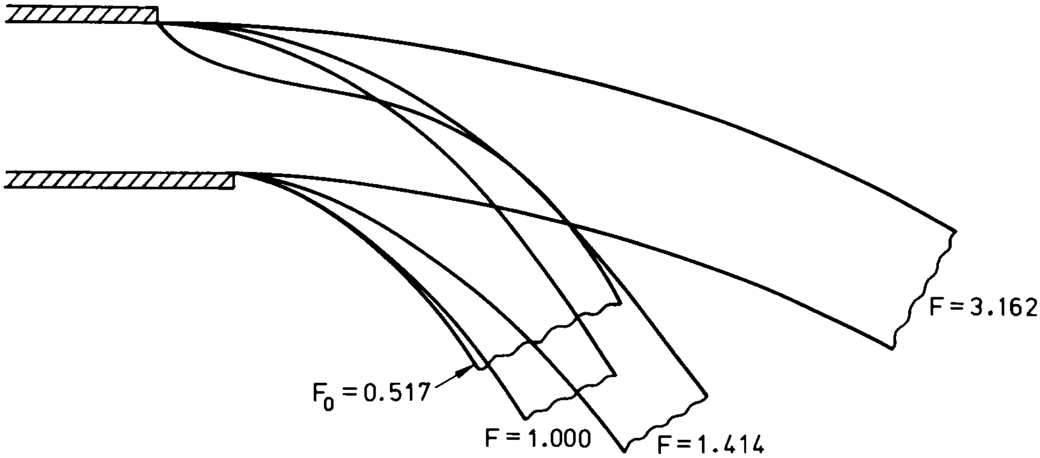

Figure 5. Underhang profile for various Froude numbers.

wall. However, there is a slight "waviness" in the upper free surface, and this corresponds to the two inflexion points discussed above. Physically, when F is close to F_0, the water particles near the upper free surface initially accelerate rapidly down on a 60° slope from the stagnation point, but soon "re-bound" on meeting those particles near the lower free surface, which are still being influenced by the lower wall. This tendency to re-bound is

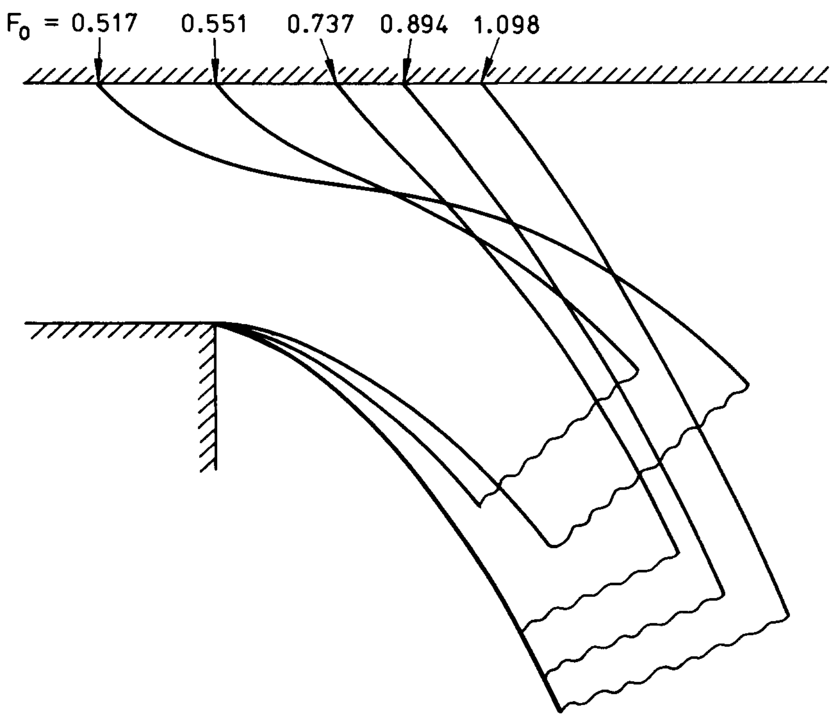

Figure 6. Stagnation-point profiles for various Froude numbers, each corresponding to a different overhang.

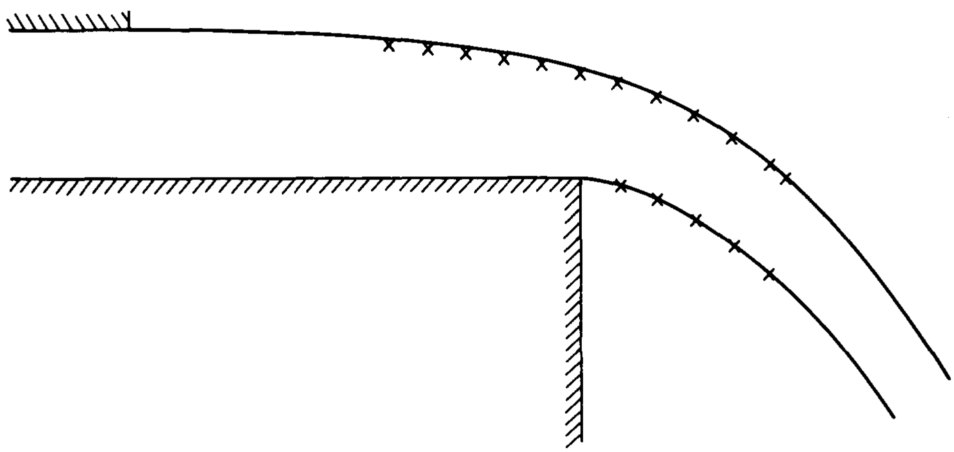

Figure 7. Comparison of $l = -2.711$ result (solid curve) with Smith and Abd-el-Malek's (crosses) solution to the waterfall problem at $F = 1$.

quickly swamped by the fall under gravity, and the second change in curvature takes place, after which the jet falls more rapidly and becomes more thin the lower is F. The re-bound phenomenon is even more apparent in the underhang case of Figure 5, since then the lower wall itself can play a more direct role as a barrier to the initial fall.

If one attempts, at any given overhang l, to reduce F below F_0, detachment will in practice simply move back along the upper wall. That is, the value of l will lessen in such a way as to maintain the Froude number at the value $F = F_0(l)$ corresponding to the new value of l. Thus the limiting flows have an interesting alternative interpretation as the flows that would actually be achieved at any Froude number F, when there is an upper wall that extends arbitrarily far to the right, but with stagnation-point detachment at $x = l$ from that upper wall, where l is determined by solving $F = F_0(l)$. Figure 6 shows a family of such flows.

Finally, let us consider an approach to the true waterfall case, in which there is no upper wall. This can be achieved by letting $l \to -\infty$ in the present formulation. In practice, this means that we must run the existing program for L values very close to unity, which involves some loss of precision. However, results were obtained for $l = -2.711$ that are almost indistinguishable from those obtained by Smith and Abd-el-Malek [4], as is shown in Figure 7 for the case when $F = 1$. Thus, the presence of an upper wall ending at about 3 slot widths upstream has an insignificant effect on the resulting waterfall.

References

[1] W.L. Chow and T. Han, Inviscid solution for the problem of free overfall, *J. Appl. Mech.* 46 (1979) 1–5.

[2] N.S. Clarke, On two dimensional inviscid flow in a waterfall, *J. Fluid Mech.* 22 (1965) 359–369.

[3] J. Geer and J.B. Keller, Slender streams, *J. Fluid Mech.* 93 (1979) 97–115.

[4] A.C. Smith and M.B. Abd-el-Malek, Hilbert's method for numerical solution from a uniform channel over a shelf, *J. Engg. Math.* 17 (1983) 27–39.

[5] E.O. Tuck, The shape of free jets of water under gravity, *J. Fluid Mech.* 76 (1976) 625–640.

[6] J.M. Vanden-Broeck and J.B. Keller, Jets rising and falling under gravity, *J. Fluid Mech.* 124 (1982) 335–346.